Water Research 171 (2020) 115401

Contents lists available at ScienceDirect

Water Research

journal homepage: www.elsevier.com/locate/watres

Aggregation and stability of nanoscale plastics in aquatic environment

Mehnaz Shams, Iftaykhairul Alam, Indranil Chowdhury*

Department of Civil & Environmental Engineering, Washington State University, Pullman, WA, 99164, USA

ARTICLE INFO

Article history:
Received 10 September 2019
Received in revised form
13 December 2019
Accepted 15 December 2019
Available online 18 December 2019

Keywords:
Polyethylene
Polystyrene
Nanoscale plastics
Aggregation
Stability

ABSTRACT

The widespread use and release of plastics in nature have raised global concerns about their impact on public health and the environment. While much research has been conducted on macro- and micro-sized plastics, the fate of nanoscale plastics remains unexplored. In this study, the aggregation kinetics and stability of polyethylene and polystyrene nanoscale plastics were investigated over a wide range of aquatic chemistries (pH, salt types (NaCl, $CaCl_2$, $MgCl_2$), ionic strength) relevant to the natural environment. Results showed that salt types and ionic strength had significant effects on the stability of both polyethylene and polystyrene nanoscale plastics, while pH had none. Aggregation and stability of both polyethylene and polystyrene nanoscale plastics in the aquatic environment followed colloidal theory (DLVO theory and Schulze-Hardy rule), similar to other colloidal particles. The critical coagulation concentration (CCC) values of polyethylene nanoscale plastics were lower for $CaCl_2$ (0.1 mM) compared to NaCl (80 mM) and $MgCl_2$ (3 mM). Similarly, CCC values of polystyrene nanospheres were 10 mM for $CaCl_2$, 800 mM for NaCl and 25 mM for $MgCl_2$. It implies that $CaCl_2$ destabilized both polyethylene and polystyrene nanoscale plastics more aggressively than NaCl and $MgCl_2$. Moreover, polystyrene nanospheres are more stable in the aquatic environment than polyethylene nanoscale plastics. However, natural organic matter improved the stability of polyethylene nanoscale plastics in water primarily due to steric repulsion, increasing CCC values to 0.4 mM, 120 mM and 8 mM for $CaCl_2$, NaCl and $MgCl_2$ respectively. Stability studies with various water conditions demonstrated that polyethylene nanoscale plastics will be fairly stable in the natural surface waters. Conversely, synthetic surface water, wastewater, seawater and groundwater rapidly destabilized polyethylene nanoscale plastics. Overall, our findings indicate that significant aqueous transport of nanoscale plastics will be possible in natural surface waters.

1. Introduction

Occurrence and accumulation of plastic materials in the environment have recently become a major concern and global environmental threat (Rillig, 2012). The most commonly detected plastics in the environment are polymers with a carbon backbone, such as polyethylene (PE), polyvinyl chloride (PVC), polypropylene (PP), polyethylene terephthalate (PET), and polystyrene (PS), (Andrady, 2011; Rochman et al., 2013; Wright et al., 2013). Among all, polyethylene and polystyrene are most used, especially in personal care products, kitchen appliances, disposable drinking cups, packaging material and thus a higher chance of finding their way into the environment (Lu et al., 2009; Rao and Geckeler, 2011) (Gausepohl and Nießner, 2001) (Beach, 1972; Gouin et al., 2015). Microbeads used in different personal care products, as exfoliants are termed as primary microplastics, as they are manufactured explicitly in the micrometer size range and for specific purposes (Von Moos et al., 2012; Zitko and Hanlon, 1991). On the other hand, secondary microplastics are formed due to the degradation of larger disposed plastics, including car tires, agricultural plastic mulch, microfibers from textiles, etc. As the usage and disposal of these plastics increased over time, the occurrence of plastics in the environment has also accelerated. Both primary microplastics, microbeads are likely to be washed down through drainage systems and into wastewater treatment plants (WWTPs) (Fendall and Sewell, 2009; Lechner and Ramler, 2015). According to a study, around 8 trillion pieces of microplastics enter the aquatic environment per day through WWTP (Rochman et al., 2015). Most current WWTPs are not designed to remove micro or nanoscale plastics entirely (Fendall and Sewell, 2009; Leslie et al., 2013) due to their size or density (Ziajahromi et al., 2016b), be released into the

---

* Corresponding author.
E-mail address: indranil.chowdhury@wsu.edu (I. Chowdhury).

https://doi.org/10.1016/j.watres.2019.115401

freshwater environment with effluent (Carr et al., 2016; Murphy et al., 2016) and end up in our drinking water, which indicates, potential consumption of nanoscale plastics by human (Fendall and Sewell, 2009; Lechner and Ramler, 2015; Leslie et al., 2013; Mary Kosuth et al., 2017). Moreover, micro or nanoscale plastics in the raw wastewater gets retained in sewage sludge (Magnusson and Norén, 2014; Ziajahromi et al., 2016a). The widespread application of this sludge to agricultural purposes is likely to pose unknown consequences to human or livestock health (Nizzetto et al., 2016a, 2016b). Irrespective of the source of entry, both primary and secondary plastics eventually break down into microplastics (Law and Thompson, 2014) via chemical, mechanical, biological, etc. processes and eventually to nanoscale plastics, through UV-radiation, mechanical abrasion, biological degradation etc.(Corcoran et al., 2009; Lambert et al., 2013; Shim et al., 2014). This has become a recent concern due to limited information on their behavior and fate in the environment. Even though there is a disagreement in the size values of different plastics, for the current study, plastics within the size range of 1 nm to 1 μm are referred to as nanoscale plastics.

Microplastics or its derivatives, similar to nanoparticles (Syberg et al., 2015), can penetrate human organs via cell barrier and cause cytotoxicity and metabolic disorders (Bothun, 2008; Lewinski et al., 2008; Liu et al., 2018; Rasch et al., 2010; Yousefi and Tufenkji, 2016; Yousefi et al., 2016). These micro and nanoscale plastics can also undergo various transformations that can influence their aggregation and deposition behavior and potentially aggravate the associated environmental hazards (Bouwmeester et al., 2015; Cózar et al., 2014; Velzeboer et al., 2014). Some previous studies have researched on the behavior of microplastics in soils and waters; however, to the best of our knowledge, the presence and impact of nanoscale plastics (<100 nm) in natural systems have been neglected which could represent a considerable future challenge for monitoring and risk assessment (Alimi et al., 2018). In the U.S., there is still a shortcoming on strict regulations on micro and nanoscale plastics, whereas in other countries the limit is so high as to be ineffective (Alimi et al., 2018; Lechner et al., 2014). Moreover, as the plastic material comes in a wide variety of sizes, forms, and types, varying in specific gravity, structure and general characteristics (Andrady, 2011; Barany et al., 2012; Cai et al., 2018; Lefèvre et al., 2009; Ohsawa et al., 1986; Pesudovs, 2000), more research needs to be conducted with a wide range of sizes and types of nanoscale plastics.

Similar to nanoparticles, nanoscale plastics are also emerging contaminants, and parallels were drawn from their detailed characteristics overview in a study (Hüffer et al., 2017). From that study, it was evident that fate research of nanoparticles can be transferred to nanoscale plastics. Especially, environmental transformation and transport, sample preparation for particle analysis and characterization techniques for nanoparticles can be applied to nanoscale plastics as well. Previous studies for engineered nanomaterials showed that aggregation with suspended solids and subsequent sedimentation is the most likely removal process for these particles in water (Praetorius et al., 2012; Quik et al., 2011, 2015). Therefore, here the early stage aggregation kinetics of polyethylene and polystyrene nanoscale plastics under various environmentally relevant solution chemistries have been investigated. These include variations in monovalent (NaCl) and divalent ($CaCl_2$ and $MgCl_2$) salt concentrations and the presence of natural organic matter (Suwannee River humic acid). As mentioned earlier, polyethylene and polystyrene are the commonly detected plastic in the environment (Lu et al., 2009; Rao and Geckeler, 2011) (Lu et al., 2009; Rao and Geckeler 2011),they were selected for the present study. Additionally, stability of polyethylene nanoscale plastics has been determined in Columbia River Water (CRW), along with synthetic surface water, groundwater, seawater and wastewater to simulate the aquatic systems. This current study on different types of plastics could serve as a fundamental framework to do more research in future with a variety of plastics.

2. Materials and methods

2.1. Materials

Polyethylene nanospheres (0.95 g/cc density, 200 nm–9900nm diameter) were purchased from Cospheric LLC (CA, USA). The surfactant used for the dispersion of the polyethylene nanoscale plastics was sodium dodecyl sulfate (SDS), an anionic surfactant OECD (2005), provided by Thermo Fisher Scientific. Carboxyl modified polystyrene latex (4% w/v, 0.028 μm) were purchased from Thermo Fisher Scientific. All aqueous solutions were prepared with Milli-Q (Deionized water $\geq$ 18 MΩ) water.

Depending on the usage, hydrophobic plastics undergo surface functionalization with different functional groups. Moreover, plastics that end up in the aquatic environment might get coated with surfactants as well. These surface modifications make plastic hydrophilic in nature and help them for dispersion. So, plastics in the environment do not remain in their pristine state. Hence, we selected our materials considering these surface modifications in the natural aquatic environment. However, our study is limited to only spherical particles and particles coated with one specific substance, whereas in actual environment, the plastics could be coated with a mixture of substances.

2.2. Preparation of nanoscale plastics dispersion

Polystyrene latex was purchased in a suspension of de-ionized water and was diluted to 40 mg/L with DI water as a stock solution for subsequent experiments. Polyethylene nanoscale plastics solution was prepared by mixing polyethylene nanoscale plastics with MQ water following the procedure used for nanomaterials (Islam et al., 2003; O'connell et al., 2002; Strano et al., 2003b). Then 0.1 wt% SDS was added to the solution. The mixture was sonicated for 30 min or until the SDS powder completely dissolved and polyethylene nanoscale plastics were in suspension. The flask was placed in a bath of ice water during sonication in order to prevent the temperature rise of the mixture. For homogenous size distribution and to remove the larger sized particles, prepared polyethylene nanoscale plastics suspension was filtered with 0.45 μm cellulose acetate filter so that the filtrate contains small size nanoscale plastics. The final concentration of the polyethylene nanoscale plastics stock solution was 40 mg L^{-}, which was quantified with the calibration curve prepared by UV–Vis spectroscopy.

2.3. Selection of surfactant for polyethylene nanoscale plastics dispersion

Due to the hydrophobic nature of polyethylene nanoscale plastics, SDS surfactant was used to disperse polyethylene nanoscale plastics (Mintenig et al., 2018). SDS is extensively used both for fundamental studies as well as in many industrial applications such as in car wash soap, engine degreasers and floor cleaners, personal care products, etc. So it is likely that they will end up in the environment similar to our polyethylene nanoscale plastics and will also interact with them (Tadros, 2006). Previous studies with engineered nanoparticles also showed that fate of nanoparticles will be highly dependent both on their released form and on the physicochemical characteristics of the receiving waterbody, which could include the presence of SDS (Collin et al., 2014; Cornelis, 2015; Goldberg et al., 2015; Louie et al., 2016; Pokhrel et al., 2014). In particular, surfactants such as sodium dodecyl sulfate (SDS) have been studied for their excellent nanotube stabilization, separation capabilities and it is also a commonly used surfactant (Islam et al., 2003; O'connell et al., 2002; Strano et al., 2003b). Moreover, SDS is commonly used as an additive for plastics to do surface functionalization (Koelmans et al., 2015, 2005; Péron et al., 2007). The production of everyday plastics would not be possible without surfactants, which are used in both emulsion and suspension polymerization production processes (Falbe, 2012).

2.4. Aquatic chemistry

Suwannee River humic acid (Standard II, International Humic Substances Society) was used to prepare the natural organic matter (NOM) suspension at a concentration of 5 mg/L (TOC). These NOMs have been previously used as model or standard substances in many aggregation, fate and transport studies. (Chen et al., 2006; Chowdhury et al., 2013, 2015; Liu et al., 2010). Calcium chloride ($CaCl_2 \cdot 2H_20$, CAS 10035048), sodium chloride (NaCl, CAS 7647-14-5) and magnesium chloride ($MgCl_2 \cdot 6H_20$, CAS 7791-18-6), were used to prepare salt solutions. 1, 10, 30, 50, 80, 100, 120 mM NaCl, 0.01, 0.05, 0.08, 0.1, 0.5, 1 mM $CaCl_2$ and 0.5, 1, 3, 4, 5 mM $MgCl_2$ were used for the experiments. To determine the isoelectric point for both nanoscale plastics, electrophoretic mobility (EPM) and zeta potential (ZP) were measured in 10 mM NaCl over a pH range from 2 to 10, using NaOH and HCl.

2.5. Characterization of nanoscale plastics

To observe the material and aggregate morphology, Tescan Vega 3 scanning electron microscope (SEM) was used to obtain SEM images (Fig. 1).

FTIR measurements were performed directly on polyethylene nanoscale plastics using attenuated total reflection (ATR) mode on a Nicolet iS50 ATR-IR with Ge crystal (Fig. S1). The FTIR analysis method uses infrared light to scan test samples and observe chemical properties.

Ultraviolet (UV)-visible spectroscopy spectra (Figs. S2 and S3) was collected using a PerkinElmer Lambda 365 UV—visible absorbance spectrophotometer to monitor both the polyethylene and polystyrene nanoscale plastics concentration and changes in light absorption properties.

Electrophoretic mobility (EPM), zeta potential (ZP) and hydrodynamic diameter (D_h) of the particles were measured using a Zetasizer Nano ZS (Malvern Instruments, Inc.) equipped with a monochromatic coherent He – Ne laser with a fixed wavelength of 633 nm.

NOM concentration was measured as total organic carbon (TOC) using a Shimadzu TOC-Vcsh total organic carbon analyzer with the non-dispersive infrared (NDIR) method.

2.6. Aggregation kinetics

Aggregation kinetics of nanoscale plastics at different aquatic chemistry conditions (salt type, IS, and presence of organic matter) was determined in terms of hydrodynamic size measurement. This change in the size of polyethylene nanoscale plastics was measured with respect to time by time-resolved dynamic light scattering (TR-DLS) (Bouchard et al., 2012). Both polyethylene and polystyrene nanoscale plastics concentration of 20 mg/L provided a strong DLS signal and therefore was used in all aggregation studies. Polyethylene nanoscale plastics solutions were filtered through a 0.45 μm cellulose acetate filter (Millipore, U.S.A) for homogeneous size distribution. Equal volumes (800 μL) of nanoscale plastics suspension and electrolyte solution (NaCl, $CaCl_2$, or $MgCl_2$) were pipetted into a quartz cuvette to achieve a specific nanoscale plastics and electrolyte concentration. The cuvette was immediately placed in the DLS instrument after bath sonicating for 5 s. The intensity of scattered light was measured at 173°, and the autocorrelation function was allowed to accumulate for 15 s during aggregation study. The hydrodynamic diameter (D_h) measurements were conducted over periods ranging from 30 to 300 min. The initial aggregation period was defined as the time period from experiment initiation (t_0) to the time when measured D_h values exceeded 1.50 $D_{h,\text{ initial}}$ (Bouchard et al., 2012). The initial aggregation rate constants (k_a) for the nanoscale plastics are proportional to the initial rate of increase of D_h with time (Chen and Elimelech, 2006):

$$k_a \propto \frac{1}{N_0}\left(\frac{dD_h(t)}{dt}\right)_{t\to 0} \tag{1}$$

where N_0 is the initial particle concentration. The particle attachment efficiency, α is used to quantify particle aggregation kinetics; it is defined as the initial aggregation rate constant (k_a), normalized by the aggregation rate constant measured under diffusion-limited (fast) conditions (Chen and Elimelech, 2006).

$$\alpha = \frac{1}{W} = \frac{k_a}{k_{a,\text{ fast}}} = \frac{\frac{1}{N_0}\left(\frac{D_h(t)}{dt}\right)_{t\to 0}}{\frac{1}{N_{0,\text{ fast}}}\left(\frac{D_h(t)}{dt}\right)_{t\to 0,\text{ fast}}} \tag{2}$$

Because the concentration of the nanoscale plastic across all samples in aggregation experiments was identical, equation (2) can be simplified (i.e., N_0 drops out) and α can be determined directly by normalizing the initial slope of the aggregation profile for a specific background solution chemistry by the initial slope under diffusion-limited (fast) conditions (Chen and Elimelech, 2006). Note that α is the inverse of the Fuchs stability ratio (W) commonly used in colloidal stability studies. Critical coagulation concentrations (CCC) of polyethylene nanoscale plastics were determined from the intersection of extrapolated lines through the diffusion and reaction limited regimes.

2.7. Derjaguin—Landau—Verwey—Overbeek (DLVO) theory

Classical Derjaguin—Landau—Verwey—Overbeek (DLVO) theory has been applied to understand the influence of electrostatic and van der Waals forces on the interaction among nanoscale plastics with and without NOM (Derjaguin, 1954; Overbeek, 1999a). The DLVO theory explains the aggregation of aqueous dispersions quantitatively and describes the force between charged surfaces interacting through a liquid medium. It combines the effects of the van der Waals attraction and the electrostatic repulsion (Gregory, 2005). DLVO interaction energies between nanoscale plastics, separated by a distance h were calculated assuming a sphere-sphere geometry by utilizing the following equations (Elimelech et al., 1997).

$$V_{el} = 2\pi\varepsilon_0\varepsilon a_p \Psi_p^2 \ln[1+\exp(-kh)] \tag{3}$$

$$V_{vdW} = -\frac{A_{131}a_p}{12h}\left[1+\frac{14h}{\lambda}\right]^{-1} \tag{4}$$

$$V_{Total} = V_{EDL} + V_{vdw} \tag{5}$$

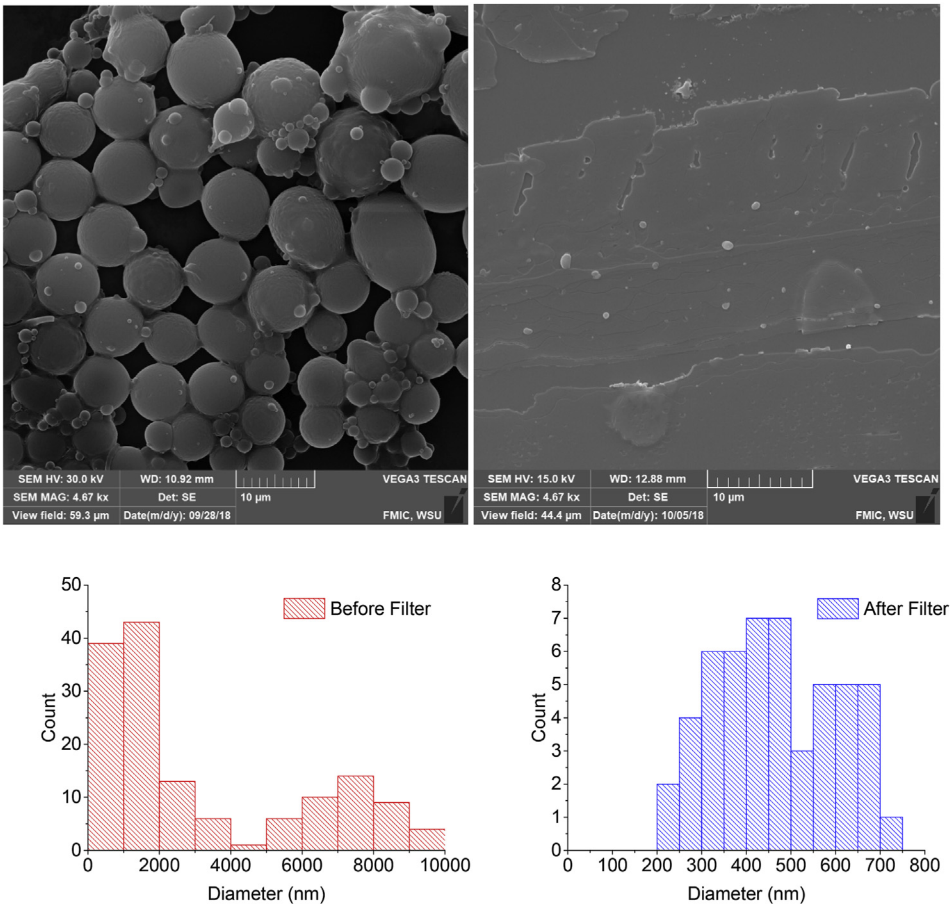

Fig. 1. SEM images and size distribution of polyethylene nanoscale plastics in MiliQ water before filter (Left) and after filter (Right). Concentration of polyethylene nanoscale plastics = 40 mg/L, the average diameter of polyethylene nanoscale plastics is found to be from 300 to 6100 nm, from 146 particles (before filter) and 200–750 nm, from 100 particles (after filter). Particle size distribution were determined considering the diameter of the spheres using ImageJ software.

$$A_{131} = \left(A_{11}{}^{½} - A_{33}{}^{½}\right)\left(A_{11}{}^{½} - A_{33}{}^{½}\right) \tag{6}$$

$$\kappa = \frac{I^{0.5}}{0.3049*10^{9}} \tag{7}$$

where.

A_{131} = Hamaker Constant (J) for two similar materials 1 (polyethylene nanoscale plastics) interacting through medium 3 (water)
A_{11} = Hamaker constant for polyethylene nanoscale plastics, 7.6×10^{-20} J
A_{33} = Hamaker constant for water, 3.7×10^{-20} J (Freitas, 1999)
k = Debye length (m^{-1})
a_p = Colloid particle radius (m)
λ = Dielectric wavelength (m)
ε_0 = Permittivity of free space (C/V/m)
ε = Dielectric constant of water
Ψ_p = Colloid surface potential (V)
I = Ionic strength (M)

Hamaker Constant, A_{131} was employed as $6.94*10^{-21}$ J in our study (Freitas, 1999). The permittivity of free space (ε_0) and dielectric constant of water (ε) were assumed to be 8.854×10^{-12} C/V/m and 78.5 respectively (Elimelech et al., 1997; Hong et al., 2009). Hydrodynamic size measured by DLS was used as particle size (α_p). Experimentally determined zeta potentials of nanoscale plastics were used in the place of surface potentials (Ψ_p). 100 nm was assumed as characteristic dielectric wavelength (λ) (Elimelech et al., 1997).

2.8. *Stability of polyethylene nanoscale plastics in different water conditions*

The stability of polyethylene nanoscale plastics in different water conditions was investigated to observe the behavior of polyethylene nanoscale plastics in complex environmental relevant conditions. Five different types of water were used. Natural surface water was collected from Columbia River Water, a point near Lower Granite Point, WA. Apart from the natural water, the behavior of polyethylene nanoscale plastics in synthetic water was also investigated. Synthetic surface water (Yip et al., 2011), groundwater (Bolster et al., 1999), and seawater (Stewart and Munjal, 1970) were prepared following recipes mentioned in the supplementary information (Tables S1 and S2). The chemical composition of the synthetic wastewater was based on secondary effluent quality from wastewater treatment plants in California as summarized in Table S3 (Boo et al., 2013). Sodium alginate (SA) and Bovine serum albumin (BSA), purchased from Sigma-Aldrich were used as model polysaccharides and protein foulant respectively for this study. Detailed characteristics of these waters are provided in the Supporting Information (Tables S1, S2, S3). Aggregation kinetics of

20 mg/L polyethylene nanoscale plastics at these water conditions was determined in terms of hydrodynamic size measurement.

2.9. Statistical analysis

Statistical testing was employed for data analysis. Two-sample t-tests for hypothesis testing were conducted using OriginPro 2016 software (OriginLab Corporation, MA) to guarantee the statistical significance of the conclusions. Probability values (P) of less than 0.05 were considered as statistically significant.

3. Results and discussion

3.1. Characterization of polyethylene nanoscale plastics

Fig. 1 contains a representative SEM image of polyethylene nanoscale plastics in MiliQ water before (left image) and after (right image) filter, from which the particle size distribution was determined using ImageJ software. The particle size distribution before the filter was determined to be from 300 to 6100 nm, from 146 particles, which is within the range of the size distribution provided by Cospheric LLC (CA, USA). After filter, larger size particles were filtered, evident from the SEM images, and the particle size distribution was determined to be from 200 to 750 nm, from 100 particles, which makes a homogeneous size distribution.

Figure S1 shows the characteristics absorbance bands for polyethylene which are located at: 2916 cm^{-1} (C–H asymmetrical stretching vibration), 2855 cm^{-1} (C–H symmetrical stretching vibration), 1475 cm^{-1} (CH_2 scissoring vibration) & 718 cm^{-1} (CH_2 rocking vibration). The 1475 cm^{-1} & 716 cm^{-1} peaks are used to identify and quantify the presence of polyethylene (D¡Amelia et al., 2016; Gulmine et al., 2002).

3.2. Electrokinetic and hydrodynamic characterization

3.2.1. Influence of pH on surface charge and size

EPM measurements using Zetasizer Nano ZS (Fig. S4b) showed that polyethylene nanoscale plastics remained highly negatively charged over the pH range from 2 to 9 (from −2.39 ± 1.22 μmcm/Vs at pH 2 to −2.44 ± 0.33 μmcm/Vs at pH 9) at 10 mM NaCl. This indicates that either polyethylene nanoscale plastics don't have any isoelectric point (IEP) (Barany et al., 2012; Lefèvre et al., 2009; Ohsawa et al., 1986), or they have isoelectric point below pH 2. Moreover, pKa for SDS is ~1.99, due to which isoelectric point was not observed at the studied pH range (Chakraborty et al., 2009; Strano et al., 2003a) and maintaining pH below 2 without sacrificing control of the IS (10 mM) was not possible.

The change of hydrodynamic diameter to different pH at 10 mM NaCl (Fig. S4a) was similar to EPM measurements, with polyethylene nanoscale plastics size remaining statistically constant from 217.95 ± 24.61 nm to 310.29 ± 165.58 nm from pH 2 to 9.

EPM measurements of polystyrene nanospheres (Fig. S5b) also showed that polystyrene nanospheres are negatively charged over the pH range from 2 to 9 (from −0.76 ± 0.10 μmcm/Vs at pH 2 to −2.52 ± 0.17 μmcm/Vs at pH 9) at 10 mM NaCl and they don't have any isoelectric point (IEP) similar to polyethylene nanoscale plastic. Absolute values of polystyrene EPMs increased from pH 2 to pH 5 (from −0.76 ± 0.10 μmcm/Vs at pH 2 to −1.93 ± 0.02 μmcm/Vs at pH 5), while EPMs remained very similar from pH 6 to 9 (−2.87 ± 0.67 μmcm/Vs to −2.52 ± 0.17 μmcm/Vs). This change in EPM with pH (Fig. S5b) is due to the dissociable functional groups on polystyrene nanospheres, similar to other carbon-based materials (Bouchard et al., 2009; Chowdhury et al., 2013; Saleh et al., 2008). The change of hydrodynamic diameter of polystyrene nanospheres (Fig. S5a), to different pH at 10 mM NaCl was similar to EPM measurements, with polystyrene hydrodynamic diameter decreasing from pH 2 to pH 5 (~3700 nm−1100 nm) as predicted by colloidal theory (Verwey and Overbeek, 1948), then remaining quite constant from pH 5 to 9 (~900 nm).

The pH in the aquatic environment usually remains between 5 and 9 (Crittenden and Montgomery Watson, 2005). As there are no notable changes in electrokinetic and hydrodynamic properties of both polyethylene and polystyrene nanoscale plastics within this range, it is likely that pH will not affect the behavior of these nanoscale plastics in the aquatic environment. Thus, the aggregation kinetics and stability of nanoscale plastics were investigated at an unadjusted pH 5 ± 0.2 in this study.

3.2.2. Influence of salt type and ionic strength

Polyethylene nanoscale plastic is highly negatively charged (EPM is −4.60 ± 0.44 μmcm/Vs and ZP is −58.7 ± 5.57 mV) in MQ water. This high negative charge indicates that polyethylene nanoscale plastics are electrically stabilized with hydrodynamic diameter of 376.36 ± 34.47 nm due to the large electrostatic repulsion between polyethylene nanoscale plastics (Gregory, 2005) EPM values of polyethylene nanoscale plastics remain highly negative (around −5.03 ± 0.19 μmcm/Vs to −3.95 ± 0.86 μmcm/Vs) at low NaCl concentration (1 mM−50 mM; Fig. 2b). EPM decreases from −3.95 ± 0.86 μmcm/Vs to −2.07 ± 0.83 μmcm/Vs when NaCl concentration was increased from 50 mM to 120 mM (Fig. 2b). The decrease in surface charge with an increase in ionic strength is due to electrical double layer compression, as predicted by DLVO theory (Elimelech et al., 1995; Verwey and Overbeek, 1948). Similar trends were observed for nanomaterials, including GO and multiwalled carbon nanotubes as well (Chowdhury et al., 2013; Saleh et al., 2008). From 1 to 50 mM NaCl, hydrodynamic diameter of polyethylene nanoscale plastics remained quite constant ~680 nm respectively (Fig. 2a). Above 50 mM NaCl, the EPM of polyethylene nanoscale plastics became less negative with IS, which resulted in a decrease in D_h from 679.22 ± 7.45 nm to 282.25 ± 165.08 nm (Fig. 2a). This observation deviates from the classical behavior predicted by DLVO theory. It is hypothesized that at higher salt levels, the dispersion forces on the ions can be dominating. When dispersion potentials are accounted for, there may be a rise to either accumulation or depletion of ions close to an interface. The dispersion potentials may change both in magnitude and sign, depending on the optical properties of the interacting surfaces, the salt solution, and the ions. This could give rise to reduced or enhanced double-layer forces and result in a reduction of apparent size (Boström et al., 2001). In surface waters, the concentration of monovalent ions (i.e., Na^+) is less than 10 mM, (Crittenden and Montgomery Watson, 2005) indicating that polyethylene nanoscale plastics will be stable in natural aquatic environments dominated by these monovalent cations.

However, Ca^{2+} and Mg^{2+} influenced the EPM and hydrodynamic diameter of polyethylene nanoscale plastics more prominently than monovalent Na^+. A notable decrease in EPM values was observed for low concentrations of $CaCl_2$ (from 0.01 mM to 0.05 mM) and $MgCl_2$ (from 0.5 to 1 mM), whereas significant decrease in EPM and subsequent electrical double layer compression was not observed for NaCl until 80 mM (Fig. 2b). This is because of higher electrical double layer compression from divalent ions with respect to monovalent ions, as described in classical colloidal theory (Elimelech et al., 1995). Ion complexation with SDS could be another mechanism for the destabilization of polyethylene nanoscale plastics in the presence of Ca^{2+} and Mg^{2+} (Sammalkorpi et al., 2009; Shen et al., 2005; Yan et al., 2010; Zhang et al., 2009). As IS increased from 0.01 mM to 1 mM for $CaCl_2$, EPM values decreased from −4.85 ± 0.16 μmcm/Vs to −3.46 ± 0.19 μmcm/Vs and as IS increased from 0.5 mM to 5 mM for $MgCl_2$, EPM values decreased

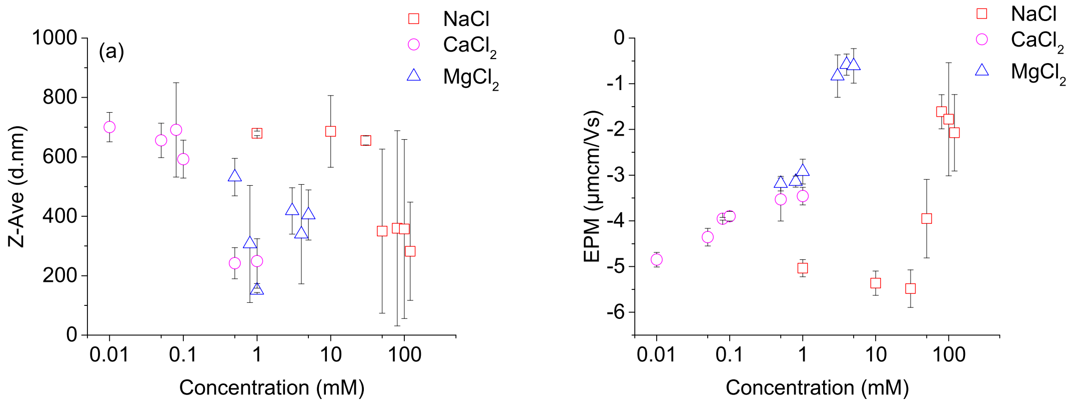

Fig. 2. (a) Hydrodynamic diameter and (b) Electrophoretic mobility (EPM) of 20 mg/L polyethylene nanoscale plastics in different electrolytes (NaCl, CaCl$_2$ and MgCl$_2$) as a function of ionic strength. Error bars indicate one standard deviation of at least three measurements.

from −3.19 ± 0.16 μmcm/Vs to −0.61 ± 0.37 μmcm/Vs (Fig. 2b). Similar trends were observed for multiwalled carbon nanotubes and graphene oxide nanomaterials in the presence of divalent cations (Chowdhury et al., 2013; Saleh et al., 2008). However, hydrodynamic diameter of polyethylene nanoscale plastics was significantly different for CaCl$_2$ and MgCl$_2$ as a function of IS. After 0.08 mM CaCl$_2$ and 3 mM MgCl$_2$, increase in hydrodynamic diameter was observed indicating greater effect of divalent cations on polyethylene nanoscale plastics aggregation (Fig. 2a).

The average hydrodynamic diameter of polystyrene nanospheres in MQ water is 43.62 ± 0.22 nm, and Electrophoretic mobility (EPM) is −4.51 ± 0.28 μmcm/Vs. This implies that polystyrene nanospheres are negatively charged in water. EPM decreases to −3.64 ± 0.41 μmcm/Vs with introduction of 10 mM NaCl, and decreased further to −2.68 ± 0.11 μmcm/Vs with increasing NaCl concentration (Fig. 3b). The decrease in surface charge with an increase in ionic strength is due to electrical double layer compression, as predicted by DLVO theory (Elimelech et al., 1995; Verwey and Overbeek, 1948). However, from 10 to 150 mM NaCl, the hydrodynamic diameter of polystyrene nanospheres remained quite constant ~42 nm (Fig. 3a) which implies that polystyrene nanospheres will be stable in natural aquatic environments even at high NaCl concentration.

Both CaCl$_2$ and MgCl$_2$ influenced the EPM of polystyrene nanospheres more aggressively than monovalent NaCl (Fig. 3b). Minor charge screening of polystyrene nanospheres was observed, even as low as 0.5 mM for both CaCl$_2$ and MgCl$_2$, while significant electrical double layer compression was not observed for NaCl until 150 mM. This is because of higher electrical double layer compression from divalent ions with respect to monovalent ions, as described in classical colloidal theory (Elimelech et al., 1995). EPMs and hydrodynamic size of polystyrene nanospheres were quite similar as a function of IS, for both CaCl$_2$ and MgCl$_2$. No notable size increase for polystyrene nanospheres was observed until 1 mM for both divalent ions (Fig. 3a), although significant charge screening was observed. After 1 mM, the hydrodynamic size of polystyrene nanospheres increased a little but not significant for both CaCl$_2$ and MgCl$_2$ (Fig. 3a).

3.2.3. Influence of natural organic matter

The effect of NOM on the electrokinetic and hydrodynamic properties of polyethylene nanoscale plastics in the presence of NaCl, CaCl$_2$ and MgCl$_2$ is reported in Table S4 in the Supporting Information. The NOM concentration was varied from 0.5 to 5 mg/L TOC. Generally, in the presence of NOM, both electrostatic repulsion and steric repulsion contribute to the stabilization of colloids (Chen and Elimelech, 2007; Jiang et al., 2017; Saleh et al., 2008; Smith et al., 2012). For the present study, NOM concentration had a negligible effect on the EPM of polyethylene nanoscale plastics in all three salt types investigated. This suggests that sorbed NOM molecules may carry the similar amount of charges to those on the surface of polyethylene nanoscale plastics (Liu et al., 2016) and electrostatic repulsion is not significant enough to cause stabilization. However, the addition of NOM reduced the hydrodynamic diameter of polyethylene nanoscale plastics under all three salt types. This indicates that steric repulsion (due to the sorption of NOM on polyethylene nanoscale plastics, which was visible by the change in surface morphology in the SEM image in Fig. S11) may be

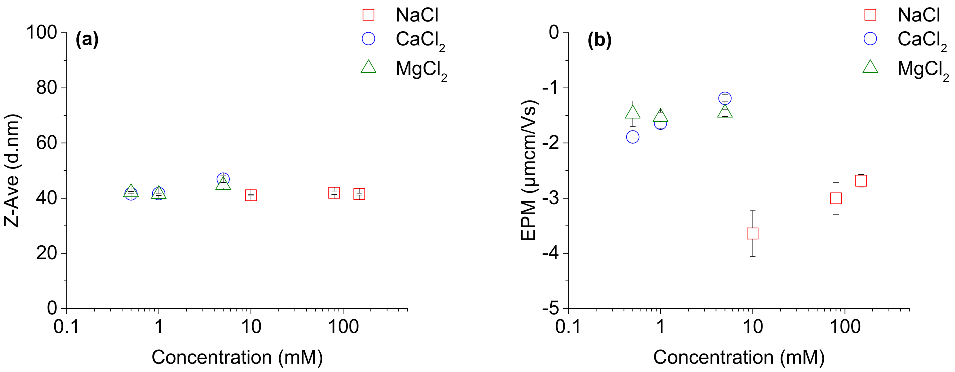

Fig. 3. (a) Hydrodynamic diameter and (b) Electrophoretic mobility (EPM) of 20 mg/L polystyrene nanospheres in different electrolytes (NaCl, CaCl$_2$ and MgCl$_2$) as a function of ionic strength. Error bars indicate one standard deviation of at least five measurements.

the dominant mechanism in polyethylene nanoscale plastics stabilization (Saleh et al., 2010).

3.3. Aggregation kinetics

3.3.1. Influence of ionic strength (IS)

Fig. S6 shows the aggregation kinetics profiles of polyethylene nanoscale plastics as a function of NaCl concentration. Attachment efficiency, α as a function of salt concentration is shown in Fig. 4a which also showed a very distinct reaction-limited and diffusion-limited regimes. This indicates that polyethylene nanoscale plastics aggregation follows Derjaguin– Landau–Verwey–Overbeek (DLVO) theory (Overbeek, 1999b). In the reaction-limited regime, α increased from approximately 12%–100% as NaCl concentration increased from 1 to 80 mM. IS beyond 80 mM did not increase α, which indicates that electrostatic repulsion between polyethylene nanoscale plastics is completely suppressed and the diffusion-limited regime starts near 80 mM NaCl (Chowdhury et al., 2012). DLVO interaction profiles between polyethylene nanoscale plastics - polyethylene nanoscale plastics are generated assuming sphere-sphere geometry (Fig. S7). Large energy barrier (>50 kT) observed at 1 mM NaCl explains the negligible aggregation of polyethylene nanoscale plastics in this condition. Increased IS (from 1 mM to 80 mM) led to reduced energy barrier, which resulted in higher aggregation as observed from aggregation experiments. Fig. 4a indicates the CCC of polyethylene nanoscale plastics is around 80 mM NaCl. Our study is the first to report the CCC of polyethylene nanoscale plastics. As a result, no direct comparison to previously published studies can be made.

The average hydrodynamic diameter of polystyrene nanospheres in MQ water is 43.62 ± 0.22 nm. The hydrodynamic diameter of polystyrene nanospheres remained stable at high ionic strength (100 mM NaCl), with a size of ~43 nm (Fig. S8). No aggregation was observed for polystyrene nanospheres even at 200 mM NaCl (Fig. S8). From the attachment efficiency values showed in Fig. 5a, calculated from the aggregation profiles (Fig. S8), we can see that CCC value of polystyrene nanospheres is 800 mM NaCl, which is 10 times greater than polyethylene nanoscale plastics CCC in NaCl. DLVO profiles of polystyrene nanospheres (Fig. S9) indicates the presence of high energy barrier even at high ionic strength (200 mM NaCl), which means greater stability of polystyrene nanospheres at high ionic strength of NaCl. From these results, it can be said that, polystyrene nanospheres are more stable than polyethylene nanoscale plastics in the presence of NaCl (Cai et al., 2018). This may be due to the aromatic content in polystyrenens structure or its surface functionalization (Bastos and De las Nieves, 1994; Sakota and Okaya, 1977; Sastri, 2010).

3.3.2. Influence of salt types

Similar to NaCl, attachment efficiency as a function of $CaCl_2$ and $MgCl_2$ salt concentration (Fig. 4b, c, 5b, 5c) also showed a very distinct reaction-limited and diffusion-limited regimes for both

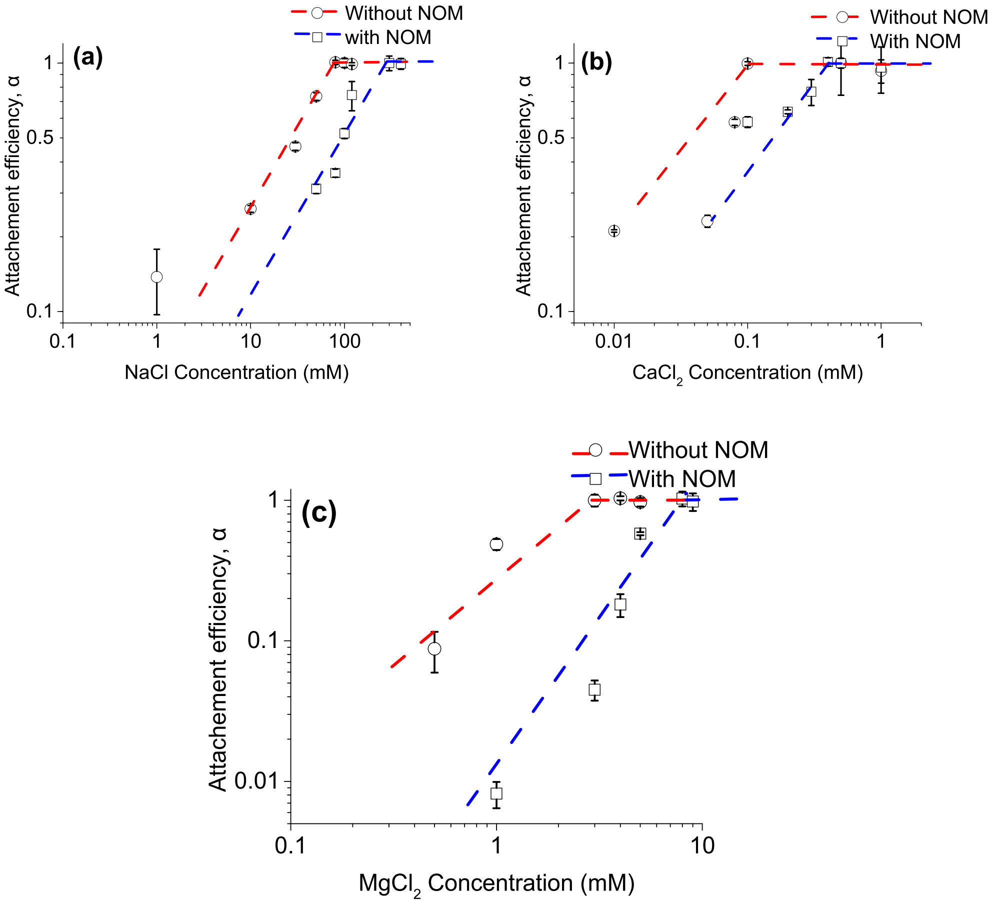

Fig. 4. Attachment efficiencies of polyethylene nanoscale plastics as a function of (a) NaCl concentration, (b) $CaCl_2$ concentration, and (c) $MgCl_2$ concentration in the presence and absence of SRHA. The dotted lines were used to determine the CCC value of polyethylene nanoscale plastics from the intersection of reaction limited and diffusion limited regimes. CCC values of polyethylene nanoscale plastics were determined from these figures as 80 mM NaCl, 0.1 mM $CaCl_2$ and 3 mM $MgCl_2$ in the absence of SRHA and 120 mM NaCl, 0.4 mM $CaCl_2$ and 8 mM $MgCl_2$ in the presence of SRHA. Error bars indicate one standard deviation of at least three measurements.

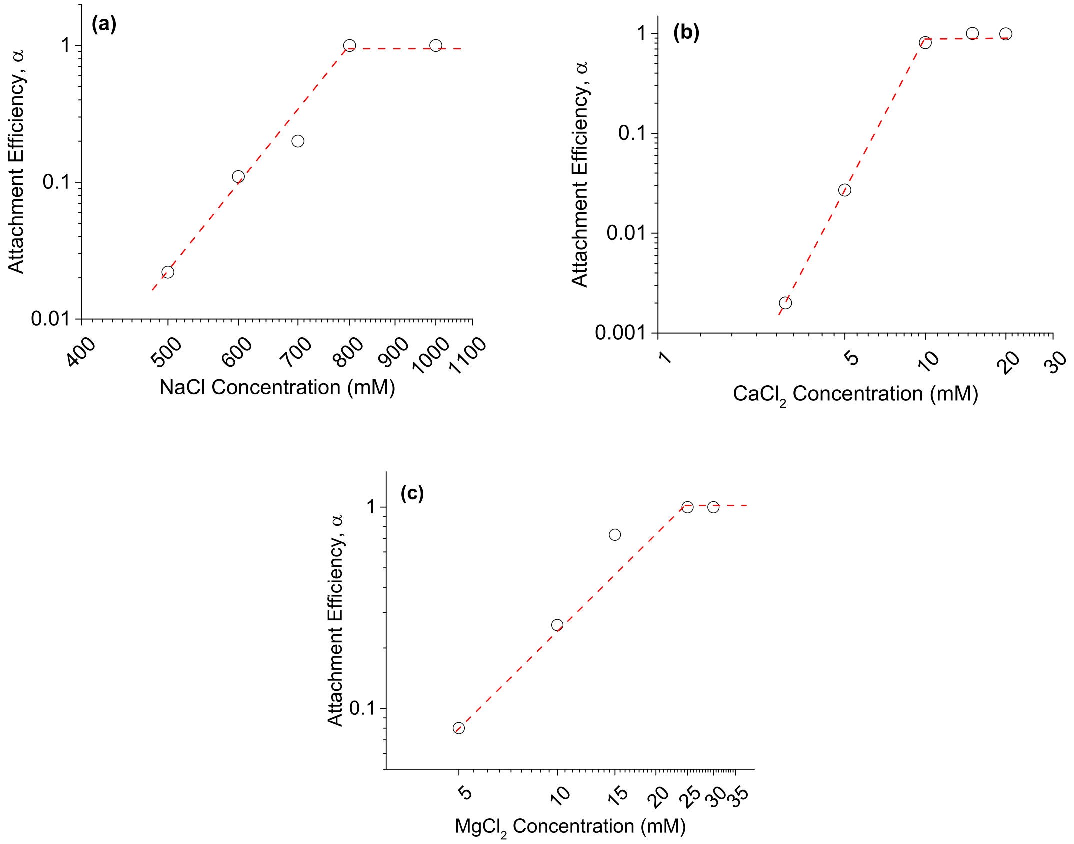

Fig. 5. Attachment efficiencies of polystyrene nanospheres as a function of (a) NaCl concentration, (b) $CaCl_2$ concentration, and (c) $MgCl_2$ concentration in the absence of SRHA. The dotted lines were used to determine the CCC value of polystyrene nanospheres from the intersection of reaction limited and diffusion limited regimes. CCC values of polystyrene nanospheres were determined from these figures as 800 mM NaCl, 10 mM $CaCl_2$ and 25 mM $MgCl_2$ in the absence of SRHA.

polyethylene and polystyrene nanoscale plastics. For $CaCl_2$, polyethylene nanoscale plastics α increased sharply from 20% to 100% with increasing IS from 0.01 to 0.1 mM. The CCC value determined from Fig. 4b is 0.1 mM $CaCl_2$, significantly lower than the CCC value for polyethylene nanoscale plastics in the presence of NaCl (Cai et al., 2018). According to the Schulze–Hardy rule, the CCC ratio for NaCl and $CaCl_2$ should be Z^{-6} for colloids with high surface charge, where Z is the valence of Ca^{2+} ions ($Z = 2$) (Gregory, 2005). In our study, the ratio of CCC values for $CaCl_2$ and NaCl is proportional to $Z^{-9.6}$, which is quite high compared with the Schulz–Hardy rule. It implies that polyethylene nanoscale plastics are sensitive to Ca^{2+} cations. This could be attributed to the specific adsorption capacity of Ca^{2+} ions, called “bridging effect” (Gutierrez et al., 2010; Nguyen and Chen, 2007; Pham et al., 2009). In a previous study, polystyrene nanoscale plastics were stable in wide ionic strength solutions of $CaCl_2$ (0.1–15 mM) (Cai et al., 2018), which again indicates that CCC value (0.1 mM $CaCl_2$) of polyethylene nanoscale plastics is notably lower than polystyrene nanoscale plastics.

On the other hand, for $MgCl_2$, minimal aggregation was observed at concentrations below 0.5 mM polyethylene nanoscale plastics α increased sharply from 10% to 100% with increasing IS from 0.5 to 3 mM. The CCC value determined from Fig. 4c is 3 mM $MgCl_2$, significantly higher than the CCC value for $CaCl_2$. This implies that Ca^{2+} is more effective than Mg^{2+} in destabilizing polyethylene nanoscale plastics in the aquatic environment. The ratio of CCC values for $MgCl_2$ and NaCl is proportional to $Z^{-4.8}$, which is reasonable as the Schulze-Hardy rule predicts a proportionality to Z^{-6} for particles of high surface charge. Also it has also been reported that a much weaker dependence on the counterion charge (Z^{-2}) exists for particles with low surface charge (Elimelech et al., 1995). Overall results suggest that, polyethylene nanoscale plastics are more sensitive to divalent cations, especially Ca^{2+} ions, than monovalent cations.

No aggregation was observed for polystyrene nanospheres even at 3 mM $CaCl_2$ and 3 mM $MgCl_2$ as the size of polystyrene nanospheres remains ~43 nm (Figs. S8b and S8c). With an increase of ionic strength for both $CaCl_2$ and $MgCl_2$, significant aggregation of polystyrene nanospheres was observed. CCC values were observed to be 10 mM for $CaCl_2$ and 25 mM for $MgCl_2$ for polystyrene nanospheres. This implies that polystyrene nanospheres are also sensitive to divalent ions especially Ca^{2+} cations following Schulz–Hardy rule. From these results, we can also predict that trivalent cations will affect aggregation and stability of nanoscale plastics in aquatic environment even more than divalent and monovalent cations according to Schulz– Hardy rule, which was observed with other nanomaterials too (Oncsik et al., 2014; Ruiz-Cabello et al., 2013; Yang et al., 2016).

In contrast to the good stability of polystyrene nanospheres and higher CCC values, polyethylene nanoscale plastics undergo obvious aggregation with low ionic strength of NaCl and $CaCl_2$. This implies that polystyrene nanospheres are more stable than polyethylene nanoscale plastics due to the surface functionalization (presence of carboxyl functional groups) of polystyrene nanospheres (Bastos and De las Nieves, 1994; Sakota and Okaya, 1977).

3.3.3. *Influence of natural organic matter*

For 80 mM NaCl, the addition of 5 mg/L (TOC) NOM reduced α from 100% to 50% (Fig. 4a), while α decreased from 100% to 60% for 0.1 mM $CaCl_2$ (Fig. 4b). The significant decrease in attachment efficiencies is attributed to non-DLVO, steric interactions imparted by the adsorbed NOM (Saleh et al., 2010). There was no significant effect of NOM concentration on the EPM of polyethylene nanoscale plastics (Table S4), indicating that there are no electrostatic interactions between polyethylene nanoscale plastics and NOM to cause polyethylene nanoscale plastics stabilization. Steric stabilization by NOM has been observed for multi-walled carbon nanotubes and aquatic colloids in a previous study (Saleh et al., 2008).

The CCC values of polyethylene nanoscale plastics in the presence of 5 mg/L (TOC) NOM were 120 mM NaCl, 1.5 times higher than observed without NOM (80 mM NaCl), 0.4 mM $CaCl_2$, 4 times higher than observed without NOM (0.1 mM $CaCl_2$) and 8 mM $MgCl_2$, 2.66 times higher than observed without NOM (3 mM $MgCl_2$). In the presence of 5 mg/L NOM, the ratio of CCC values between $CaCl_2$ and NaCl was proportional to Z^{-8}, which is quite close to what was observed in the absence of NOM. Similarly, the ratio of CCC values between $MgCl_2$ and NaCl was proportional to Z^{-4}, which is also quite close to what was observed in without NOM.

3.4. Stability of polyethylene nanoscale plastics in various water conditions

Initial aggregation studies measure the stability of nanomaterials over concise time frames.

3.4.1. Aggregation kinetics

Aggregation kinetics of polyethylene nanoscale plastics were explored in five different types of waters for 60 min to determine the initial stability of polyethylene nanoscale plastics (Fig. S12). Natural environment is a very complex ecosystem. So, we mainly used synthetic waters to simulate engineered aquatic environments and to understand the fundamental behavior of these nanoscale plastics. However, we did use Columbia River Water as our natural water to observe the changes in the behavior of these nanoscale plastics in natural environment, compared to an engineered environment. Aggregation of polyethylene nanoscale plastics was not observed in Columbia River Water due to low concentration of Ca^{2+} (4×10^{-4} mM), Na^{+} (0.17 mM), Mg^{2+} (0.05 mM) and the presence of substantial NOM (22.05 mg/L TOC) indicating that polyethylene nanoplastics will be highly stable in natural river water. On the other hand, surface water without NOM destabilized polyethylene nanoscale plastics as it contained 0.33 mM Ca^{2+}, which is well above the CCC values of polyethylene nanoscale plastics in $CaCl_2$ (0.1 mM). Seawater also destabilized polyethylene nanoscale plastics but faster compared to surface water. Synthetic seawater contained 10 mM Ca^{2+}, 500 mM Na^{+} and 54.4 mM Mg^{2+} all of which are well above the CCC values of polyethylene nanoscale plastics in $CaCl_2$, NaCl and $MgCl_2$. Synthetic groundwater and wastewater contained 0.68 mM Ca^{2+} and 0.5 mM Ca^{2+} respectively which is also well above the CCC values of polyethylene nanoscale plastics in $CaCl_{2,}$ and this caused significant aggregation of polyethylene nanoscale plastics in groundwater and wastewater as well. Overall the study indicates that polyethylene nanoscale plastics aggregation will be dominated by divalent ions, especially $CaCl_2$ and the presence of NOM.

4. Conclusions

The colloidal stability of polyethylene and polystyrene nanoscale plastics in environmentally relevant conditions was investigated in this study. It was found in this study that pH will have a negligible effect on the fate and transport of nanoscale plastics in the aquatic environment. Results indicate that polystyrene plastics are more stable compared to polyethylene nanoscale plastics, even at high ionic strength. We also found that divalent ions, especially $CaCl_2$, play significant role in the destabilization while adding NOM can increase the stability of nanoscale plastics. From the initial aggregation kinetics data, it can be anticipated that most of polyethylene nanoscale plastics will settle out during the wastewater treatment process, and end up in biosolids, sludge, and ultimately landfills and as fertilizer. Whereas, for polystyrene, heteroaggregation with other suspended particles would be necessary for the plastics to settle due to their density. However, significant aqueous transport of these nanoscale plastics will be possible in natural surface water. Therefore, it is imperative that different organizations, impose laws and regulations to limit or prevent the use of microplastics in commercial products, and at the same time, people should be educated on the proper management of plastic waste and importance of plastic recycling. This fundamental colloidal study with polyethylene and polystyrene nanoscale plastics could serve as a basis to do more future research with other nanoscale plastics.

Declaration of competing interest

The authors declare that they have no known competing financial interests or personal relationships that could have appeared to influence the work reported in this paper.

Acknowledgements

This work was supported by US Geological Survey grant via State of Washington Water Research Center. This work was also supported New Facutly Award and Startup grant from Washington State University.

Appendix A. Supplementary data

Supplementary data to this article can be found online at https://doi.org/10.1016/j.watres.2019.115401.

References

D¡Amelia, R.P., Gentile, S., Nirode, W.F., Huang, L., 2016. Quantitative analysis of copolymers and blends of polyvinyl acetate (PVAc) using fourier transform infrared spectroscopy (FTIR) and elemental analysis (EA). World Journal of Chemical Education 4 (2), 25–31.

Alimi, O.S., Farner Budarz, J., Hernandez, L.M., Tufenkji, N., 2018. Microplastics and nanoplastics in aquatic environments: aggregation, deposition, and enhanced contaminant transport. Environ. Sci. Technol. 52 (4), 1704–1724.

Andrady, A.L., 2011. Microplastics in the marine environment. Mar. Pollut. Bull. 62 (8), 1596–1605.

Barany, S., Nagy, M., Skvarla, J., 2012. Electrokinetic potential of polystyrene particles in polyelectrolyte and polyelectrolyte mixtures solutions. Colloid. Surf. Physicochem. Eng. Asp. 413, 200–207.

Bastos, D., De las Nieves, F., 1994. Colloidal stability of sulfonated polystyrene model colloids. Correlation with electrokinetic data. Colloid Polym. Sci. 272 (5), 592–597.

Beach, W.J., 1972. Skin Cleaner. Google Patents.

Bolster, C.H., Mills, A., Hornberger, G., Herman, J., 1999. Spatial distribution of deposited bacteria following miscible displacement experiments in intact cores. Water Resour. Res. 35 (6), 1797–1807.

Boo, C., Elimelech, M., Hong, S., 2013. Fouling control in a forward osmosis process integrating seawater desalination and wastewater reclamation. J. Membr. Sci. 444, 148–156.

Boström, M., Williams, D.R.M., Ninham, B., 2001. Specific Ion Effects: Why DLVO Theory Fails for Biology and Colloid Systems.

Bothun, G.D., 2008. Hydrophobic silver nanoparticles trapped in lipid bilayers: size distribution, bilayer phase behavior, and optical properties. J. Nanobiotechnol. 6 (1), 13.

Bouchard, D., Ma, X., Isaacson, C., 2009. Colloidal properties of aqueous fullerenes: isoelectric points and aggregation kinetics of C60 and C60 derivatives. Environ. Sci. Technol. 43 (17), 6597–6603.

Bouchard, D., Zhang, W., Powell, T., Rattanaudompol, U.-s., 2012. Aggregation kinetics and transport of single-walled carbon nanotubes at low surfactant concentrations. Environ. Sci. Technol. 46 (8), 4458–4465.

Bouwmeester, H., Hollman, P.C., Peters, R.J., 2015. Potential health impact of environmentally released micro-and nanoplastics in the human food production chain: experiences from nanotoxicology. Environ. Sci. Technol. 49 (15), 8932–8947.

Cai, L., Hu, L., Shi, H., Ye, J., Zhang, Y., Kim, H., 2018a. Effects of inorganic ions and natural organic matter on the aggregation of nanoplastics. Chemosphere 197, 142–151.

Carr, S.A., Liu, J., Tesoro, A.G., 2016. Transport and fate of microplastic particles in wastewater treatment plants. Water Res. 91, 174–182.

Chakraborty, S., Shukla, D., Jain, A., Mishra, B., Singh, S., 2009. Assessment of solubilization characteristics of different surfactants for carvedilol phosphate as a function of pH. J. Colloid Interface Sci. 335 (2), 242–249.

Chen, K.L., Elimelech, M., 2006. Aggregation and deposition kinetics of fullerene (C60) nanoparticles. Langmuir 22 (26), 10994–11001.

Chen, K.L., Elimelech, M., 2007. Influence of humic acid on the aggregation kinetics of fullerene (C60) nanoparticles in monovalent and divalent electrolyte solutions. J. Colloid Interface Sci. 309 (1), 126–134.

Chen, K.L., Mylon, S.E., Elimelech, M., 2006. Aggregation kinetics of alginate-coated hematite nanoparticles in monovalent and divalent electrolytes. Environ. Sci. Technol. 40 (5), 1516–1523.

Chowdhury, I., Duch, M.C., Gits, C.C., Hersam, M.C., Walker, S.L., 2012. Impact of synthesis methods on the transport of single walled carbon nanotubes in the aquatic environment. Environ. Sci. Technol. 46 (21), 11752–11760.

Chowdhury, I., Duch, M.C., Mansukhani, N.D., Hersam, M.C., Bouchard, D., 2013. Colloidal properties and stability of graphene oxide nanomaterials in the aquatic environment. Environ. Sci. Technol. 47 (12), 6288–6296.

Chowdhury, I., Mansukhani, N.D., Guiney, L.M., Hersam, M.C., Bouchard, D., 2015. Aggregation and stability of reduced graphene oxide: complex roles of divalent cations, pH, and natural organic matter. Environ. Sci. Technol. 49 (18), 10886–10893.

Collin, B., Auffan, M., Johnson, A.C., Kaur, I., Keller, A.A., Lazareva, A., Lead, J.R., Ma, X., Merrifield, R.C., Svendsen, C., 2014. Environmental release, fate and ecotoxicological effects of manufactured ceria nanomaterials. Environ. Sci.: Nano 1 (6), 533–548.

Corcoran, P.L., Biesinger, M.C., Grifi, M., 2009. Plastics and beaches: a degrading relationship. Mar. Pollut. Bull. 58 (1), 80–84.

Cornelis, G., 2015. Fate descriptors for engineered nanoparticles: the good, the bad, and the ugly. Environ. Sci.: Nano 2 (1), 19–26.

Cózar, A., Echevarría, F., González-Gordillo, J.I., Irigoien, X., Úbeda, B., Hernández-León, S., Palma, Á.T., Navarro, S., García-de-Lomas, J., Ruiz, A., 2014. Plastic debris in the open ocean. Proc. Natl. Acad. Sci. 111 (28), 10239–10244.

Crittenden, J.C., Montgomery Watson, H., 2005. Water Treatment Principles and Design. John Wiley and Sons, Inc., Hoboken, N.J.

Derjaguin, B., 1954. A theory of the heterocoagulation, interaction and adhesion of dissimilar particles in solutions of electrolytes. Discuss. Faraday Soc. 18, 85–98.

Elimelech, M., Gregory, J., Jia, X., Williams, R.A., 1995. Particle Deposition and Aggregation: Measurement, Modeling and Simulation.

Elimelech, M., Gregory, J., Jia, X., Williams, R., 1997. Particle deposition and aggregation, measurement, modeling and simulation. Colloid. Surf. Physicochem. Eng. Asp. 1 (125), 93–94.

Falbe, J., 2012. Surfactants in Consumer Products: Theory, Technology and Application. Springer Berlin Heidelberg.

Fendall, L.S., Sewell, M.A., 2009. Contributing to marine pollution by washing your face: microplastics in facial cleansers. Mar. Pollut. Bull. 58 (8), 1225–1228.

Freitas, R.A., 1999. Nanomedicine, Volume I: Basic Capabilities. Landes Bioscience Georgetown, TX.

Gausepohl, H., Nießner, N., 2001. In: Buschow, K.H.J., Cahn, R.W., Flemings, M.C., Ilschner, B., Kramer, E.J., Mahajan, S., Veyssière, P. (Eds.), Encyclopedia of Materials: Science and Technology. Elsevier, Oxford, pp. 7735–7741.

Goldberg, E., Scheringer, M., Bucheli, T.D., Hungerbühler, K., 2015. Prediction of nanoparticle transport behavior from physicochemical properties: machine learning provides insights to guide the next generation of transport models. Environ. Sci.: Nano 2 (4), 352–360.

Gouin, T., Avalos, J., Brunning, I., Brzuska, K., de Graaf, J., Kaumanns, J., Koning, T., Meyberg, M., Rettinger, K., Schlatter, H., 2015. Use of micro-plastic beads in cosmetic products in Europe and their estimated emissions to the North Sea environment. SOFW J. (Seifen Ole Fette Wachse) 141 (4), 40–46.

Gregory, J., 2005. Particles in Water: Properties and Processes. CRC Press.

Gulmine, J.V., Janissek, P.R., Heise, H.M., Akcelrud, L., 2002. Polyethylene characterization by FTIR. Polym. Test. 21 (5), 557–563.

Gutierrez, L., Mylon, S.E., Nash, B., Nguyen, T.H., 2010. Deposition and aggregation kinetics of rotavirus in divalent cation solutions. Environ. Sci. Technol. 44 (12), 4552–4557.

Hong, Y., Honda, R.J., Myung, N.V., Walker, S.L., 2009. Transport of iron-based nanoparticles: role of magnetic properties. Environ. Sci. Technol. 43 (23), 8834–8839.

Hüffer, T., Praetorius, A., Wagner, S., von der Kammer, F., Hofmann, T., 2017. Microplastic Exposure Assessment in Aquatic Environments: Learning from Similarities and Differences to Engineered Nanoparticles. ACS Publications.

Islam, M., Rojas, E., Bergey, D., Johnson, A., Yodh, A., 2003. High weight fraction surfactant solubilization of single-wall carbon nanotubes in water. Nano Lett. 3 (2), 269–273.

Jiang, Y., Raliya, R., Liao, P., Biswas, P., Fortner, J.D., 2017. Graphene oxides in water: assessing stability as a function of material and natural organic matter properties. Environ. Sci.: Nano 4 (7), 1484–1493.

Koelmans, A.A., Besseling, E., Shim, W.J., 2015. In: Bergmann, M., Gutow, L., Klages, M. (Eds.), Marine Anthropogenic Litter. Springer International Publishing, Cham, pp. 325–340.

Lambert, S., Sinclair, C.J., Bradley, E.L., Boxall, A.B., 2013. Effects of environmental conditions on latex degradation in aquatic systems. Sci. Total Environ. 447, 225–234.

Law, K.L., Thompson, R.C., 2014. Microplastics in the seas. Science 345 (6193), 144–145.

Lechner, A., Ramler, D., 2015. The discharge of certain amounts of industrial microplastic from a production plant into the River Danube is permitted by the Austrian legislation. Environ. Pollut. 200, 159–160.

Lechner, A., Keckeis, H., Lumesberger-Loisl, F., Zens, B., Krusch, R., Tritthart, M., Glas, M., Schludermann, E., 2014. The Danube so colourful: a potpourri of plastic litter outnumbers fish larvae in Europe's second largest river. Environ. Pollut. 188, 177–181.

Lefèvre, G., Čerović, L., Milonjić, S., Fédoroff, M., Finne, J., Jaubertie, A., 2009. Determination of isoelectric points of metals and metallic alloys by adhesion of latex particles. J. Colloid Interface Sci. 337 (2), 449–455.

Leslie, H., Van Velzen, M., Vethaak, A., 2013. Microplastic Survey of the Dutch Environment. Novel Data Set of Microplastics in North Sea Sediments, Treated Wastewater Effluents and Marine Biota.

Lewinski, N., Colvin, V., Drezek, R., 2008. Cytotoxicity of nanoparticles. Small 4 (1), 26–49.

Liu, X., Wazne, M., Han, Y., Christodoulatos, C., Jasinkiewicz, K.L., 2010. Effects of natural organic matter on aggregation kinetics of boron nanoparticles in monovalent and divalent electrolytes. J. Colloid Interface Sci. 348 (1), 101–107.

Liu, W., Zhao, X., Cai, Z., Han, B., Zhao, D., 2016. Aggregation and stabilization of multiwalled carbon nanotubes in aqueous suspensions: influences of carboxymethyl cellulose, starch and humic acid. RSC Adv. 6 (71), 67260–67270.

Liu, X., Tian, X., Xu, X., Lu, J., 2018. Design of a phosphinate-based bioluminescent probe for superoxide radical anion imaging in living cells. Luminescence 33 (6), 1101–1106.

Louie, S.M., Tilton, R.D., Lowry, G.V., 2016. Critical review: impacts of macromolecular coatings on critical physicochemical processes controlling environmental fate of nanomaterials. Environ. Sci.: Nano 3 (2), 283–310.

Lu, S., Qu, R., Forcada, J., 2009. Preparation of magnetic polymeric composite nanoparticles by seeded emulsion polymerization. Mater. Lett. 63 (9–10), 770–772.

Magnusson, K., Norén, F., 2014. Screening of Microplastic Particles in and Down-Stream a Wastewater Treatment Plant.

Mary Kosuth, E.V.W., Mason, Sherri A., Tyree, Christopher, Morrison, Dan, 2017. Synthetic Polymer Contamination in Global Drinking Water.

Mintenig, S.M., Bäuerlein, P.S., Koelmans, A.A., Dekker, S.C., van Wezel, A.P., 2018. Closing the gap between small and smaller: towards a framework to analyse nano- and microplastics in aqueous environmental samples. Environ. Sci.: Nano 5 (7), 1640–1649.

Murphy, F., Ewins, C., Carbonnier, F., Quinn, B., 2016. Wastewater treatment works (WwTW) as a source of microplastics in the aquatic environment. Environ. Sci. Technol. 50 (11), 5800–5808.

Nguyen, T.H., Chen, K.L., 2007. Role of divalent cations in plasmid DNA adsorption to natural organic matter-coated silica surface. Environ. Sci. Technol. 41 (15), 5370–5375.

Nizzetto, L., Futter, M., Langaas, S., 2016a. Are Agricultural Soils Dumps for Microplastics of Urban Origin? ACS Publications.

Nizzetto, L., Langaas, S., Futter, M., 2016b. Pollution: do microplastics spill on to farm soils? Nature 537, 488.

O'connell, M.J., Bachilo, S.M., Huffman, C.B., Moore, V.C., Strano, M.S., Haroz, E.H., Rialon, K.L., Boul, P.J., Noon, W.H., Kittrell, C., 2002. Band gap fluorescence from individual single-walled carbon nanotubes. Science 297 (5581), 593–596.

OECD, 2005. SIDS Initial Assessment Report for SIAM 5. Sodium dodecyl sulphate, p. 5 (CAS No: 151-21-3).

Ohsawa, K., Murata, M., Ohshima, H., 1986. Zeta potential and surface charge density of polystyrene-latex; comparison with synaptic vesicle and brush border membrane vesicle. Colloid Polym. Sci. 264 (12), 1005–1009.

Oncsik, T., Trefalt, G., Csendes, Z., Szilagyi, I., Borkovec, M., 2014. Aggregation of negatively charged colloidal particles in the presence of multivalent cations. Langmuir 30 (3), 733–741.

Overbeek, T., 1999a. DLVO Theory-Milestone of 20th Century Colloid Science-Preface. ELSEVIER SCIENCE, AMSTERDAM, NETHERLANDS. BV PO BOX 211, 1000 AE.

Overbeek, T., 1999b. DLVO theory - milestone of 20th century colloid science - Preface. Adv. Colloid Interface Sci. 83 (1–3), IX–XI.

Péron, N., Mészáros, R., Varga, I., Gilányi, T., 2007. Competitive adsorption of sodium dodecyl sulfate and polyethylene oxide at the air/water interface. J. Colloid Interface Sci. 313 (2), 389–397.

Pesudovs, D., 2000. Know Your Plastics.

Pham, M., Mintz, E.A., Nguyen, T.H., 2009. Deposition kinetics of bacteriophage MS2 to natural organic matter: role of divalent cations. J. Colloid Interface Sci. 338 (1), 1–9.

Pokhrel, L.R., Dubey, B., Scheuerman, P.R., 2014. Natural water chemistry (dissolved organic carbon, pH, and hardness) modulates colloidal stability, dissolution, and antimicrobial activity of citrate functionalized silver nanoparticles. Environ. Sci.: Nano 1 (1), 45–54.

Praetorius, A., Scheringer, M., Hungerbühler, K., 2012. Development of environmental fate models for engineered nanoparticles—a case study of TiO2 nanoparticles in the rhine river. Environ. Sci. Technol. 46 (12), 6705–6713.

Quik, J.T.K., Vonk, J.A., Hansen, S.F., Baun, A., Van De Meent, D., 2011. How to assess exposure of aquatic organisms to manufactured nanoparticles? Environ. Int. 37 (6), 1068–1077.

Quik, J.T.K., de Klein, J.J.M., Koelmans, A.A., 2015. Spatially explicit fate modelling of nanomaterials in natural waters. Water Res. 80, 200–208.

Rao, J.P., Geckeler, K.E., 2011. Polymer nanoparticles: preparation techniques and size-control parameters. Prog. Polym. Sci. 36 (7), 887–913.

Rasch, M.R., Rossinyol, E., Hueso, J.L., Goodfellow, B.W., Arbiol, J., Korgel, B.A., 2010. Hydrophobic gold nanoparticle self-assembly with phosphatidylcholine lipid: membrane-loaded and janus vesicles. Nano Lett. 10 (9), 3733–3739.

Rillig, M.C., 2012. Microplastic in Terrestrial Ecosystems and the Soil? ACS Publications.

Rochman, C.M., Hoh, E., Hentschel, B.T., Kaye, S., 2013. Long-term field measurement of sorption of organic contaminants to five types of plastic pellets: implications for plastic marine debris. Environ. Sci. Technol. 47 (3), 1646–1654.

Rochman, C.M., Kross, S.M., Armstrong, J.B., Bogan, M.T., Darling, E.S., Green, S.J., Smyth, A.R., Veríssimo, D., 2015. Scientific Evidence Supports a Ban on Microbeads. ACS Publications.

Ruiz-Cabello, F.J.M., Trefalt, G., Csendes, Z., Sinha, P., Oncsik, T., Szilagyi, I., Maroni, P., Borkovec, M., 2013. Predicting aggregation rates of colloidal particles from direct force measurements. J. Phys. Chem. B 117 (39), 11853–11862.

Sakota, K., Okaya, T., 1977. Electrolyte stability of carboxylated latexes prepared by several polymerization processes. J. Appl. Polym. Sci. 21 (4), 1025–1034.

Saleh, N.B., Pfefferle, L.D., Elimelech, M., 2008. Aggregation kinetics of multiwalled carbon nanotubes in aquatic systems: measurements and environmental implications. Environ. Sci. Technol. 42 (21), 7963–7969.

Saleh, N.B., Pfefferle, L.D., Elimelech, M., 2010. Influence of biomacromolecules and humic acid on the aggregation kinetics of single-walled carbon nanotubes. Environ. Sci. Technol. 44 (7), 2412–2418.

Sammalkorpi, M., Karttunen, M., Haataja, M., 2009. Ionic surfactant aggregates in saline solutions: sodium dodecyl sulfate (SDS) in the presence of excess sodium chloride (NaCl) or calcium chloride (CaCl2). J. Phys. Chem. B 113 (17), 5863–5870.

Sastri, V.R., 2010. Plastics in Medical Devices: Properties, Requirements and Applications. Elsevier Science.

Shen, Q., Wei, H., Wang, L., Zhou, Y., Zhao, Y., Zhang, Z., Wang, D., Xu, G., Xu, D., 2005. Crystallization and aggregation behaviors of calcium carbonate in the presence of poly (vinylpyrrolidone) and sodium dodecyl sulfate. J. Phys. Chem. B 109 (39), 18342–18347.

Shim, W., Song, Y., Hong, S., Jang, M., Han, G., Jung, S., 2014. Producing Fragmented Micro-and Nano-Sized Expanded Polystyrene Particles with an Accelerated Mechanical Abrasion Experiment, pp. 11–15.

Smith, B., Yang, J., Bitter, J.L., Ball, W.P., Fairbrother, D.H., 2012. Influence of surface oxygen on the interactions of carbon nanotubes with natural organic matter. Environ. Sci. Technol. 46 (23), 12839–12847.

Stewart, P.B., Munjal, P.K., 1970. Solubility of carbon dioxide in pure water, synthetic sea water, and synthetic sea water concentrates at-5. deg. to 25. deg. and 10-to 45-atm. pressure. J. Chem. Eng. Data 15 (1), 67–71.

Strano, M.S., Huffman, C.B., Moore, V.C., O'Connell, M.J., Haroz, E.H., Hubbard, J., Miller, M., Rialon, K., Kittrell, C., Ramesh, S., 2003a. Reversible, band-gap-selective protonation of single-walled carbon nanotubes in solution. J. Phys. Chem. B 107 (29), 6979–6985.

Strano, M.S., Moore, V.C., Miller, M.K., Allen, M.J., Haroz, E.H., Kittrell, C., Hauge, R.H., Smalley, R., 2003b. The role of surfactant adsorption during ultrasonication in the dispersion of single-walled carbon nanotubes. J. Nanosci. Nanotechnol. 3 (1–2), 81–86.

Syberg, K., Khan, F.R., Selck, H., Palmqvist, A., Banta, G.T., Daley, J., Sano, L., Duhaime, M.B., 2015. Microplastics: addressing ecological risk through lessons learned. Environ. Toxicol. Chem. 34 (5), 945–953.

Tadros, T.F., 2006. Applied Surfactants: Principles and Applications. John Wiley & Sons.

Velzeboer, I., Kwadijk, C., Koelmans, A., 2014. Strong sorption of PCBs to nanoplastics, microplastics, carbon nanotubes, and fullerenes. Environ. Sci. Technol. 48 (9), 4869–4876.

Verwey, E., Overbeek, J.T.G., 1948. Theory of Stability of Lyophobic Colloids. Elsevier Publishing" Co, Amsterdam Holland.

Von Moos, N., Burkhardt-Holm, P., Köhler, A., 2012. Uptake and effects of microplastics on cells and tissue of the blue mussel Mytilus edulis L. after an experimental exposure. Environ. Sci. Technol. 46 (20), 11327–11335.

Wright, S.L., Thompson, R.C., Galloway, T.S., 2013. The physical impacts of microplastics on marine organisms: a review. Environ. Pollut. 178, 483–492.

Yan, H., Yuan, S.-L., Xu, G.-Y., Liu, C.-B., 2010. Effect of Ca2+ and Mg2+ ions on surfactant solutions investigated by molecular dynamics simulation. Langmuir 26 (13), 10448–10459.

Yang, K., Chen, B., Zhu, X., Xing, B., 2016. Aggregation, adsorption, and morphological transformation of graphene oxide in aqueous solutions containing different metal cations. Environ. Sci. Technol. 50 (20), 11066–11075.

Yip, N.Y., Tiraferri, A., Phillip, W.A., Schiffman, J.D., Hoover, L.A., Kim, Y.C., Elimelech, M., 2011. Thin-film composite pressure retarded osmosis membranes for sustainable power generation from salinity gradients. Environ. Sci. Technol. 45 (10), 4360.

Yousefi, N., Tufenkji, N., 2016. Probing the interaction between nanoparticles and lipid membranes by quartz crystal microbalance with dissipation monitoring. Frontiers in chemistry 4, 46.

Yousefi, N., Wargenau, A., Tufenkji, N., 2016. Toward more free-floating model cell membranes: method development and application to their interaction with nanoparticles. ACS Appl. Mater. Interfaces 8 (23), 14339–14348.

Zhang, Y., Chen, Y., Westerhoff, P., Crittenden, J., 2009. Impact of natural organic matter and divalent cations on the stability of aqueous nanoparticles. Water Res. 43 (17), 4249–4257.

Ziajahromi, S., Neale, P.A., Leusch, F.D., 2016a. Wastewater Treatment Plant Effluent as a Source of Microplastics: Review of the Fate, Chemical Interactions and Potential Risks to Aquatic Organisms. Water Science and Technology wst2016414.

Ziajahromi, S., Neale, P.A., Leusch, F.D.L., 2016b. Wastewater treatment plant effluent as a source of microplastics: review of the fate, chemical interactions and potential risks to aquatic organisms. Water Sci. Technol. 74 (10), 2253–2269.

Zitko, V., Hanlon, M., 1991. Another source of pollution by plastics: skin cleaners with plastic scrubbers. Mar. Pollut. Bull. 22 (1), 41–42.